

# Multireference Driven Similarity Renormalization Group: A Second-Order Perturbative Analysis

Chenyang Li<sup>†</sup> and Francesco A. Evangelista<sup>\*,‡</sup>

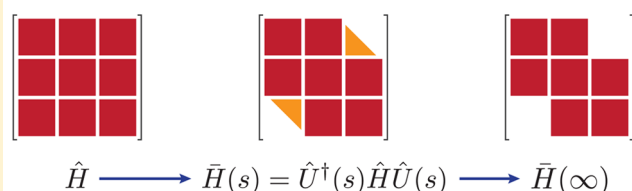
<sup>†</sup>Department of Chemistry and Center for Computational Quantum Chemistry, University of Georgia, Athens, Georgia 30602, United States

<sup>‡</sup>Department of Chemistry and Cherry L. Emerson Center for Scientific Computation, Emory University, Atlanta, Georgia 30322, United States

## S Supporting Information

**ABSTRACT:** We introduce a multireference version of the driven similarity renormalization group (DSRG) approach [Evangelista, F. A. *J. Chem. Phys.* **2014**, *141*, 054109] based on a generalized reference wave function and operator normal ordering [Kutzelnigg, W.; Mukherjee, D. *J. Chem. Phys.* **1997**, *107*, 432]. We perform a perturbative analysis of the corresponding equations at second order and derive a novel multireference perturbation theory, termed DSRG-MRPT2. The DSRG-MRPT2 energy equation can be written in a simple and compact form and can be solved via a noniterative procedure that requires at most the three-body density cumulant of the reference. Importantly, even at the perturbation level, the multireference DSRG is free from the intruder-state problem. We propose an optimal range of the DSRG flow parameter that consistently yields reliable potential energy curves with minimal nonparallelism error. We find that the DSRG-MRPT2 can describe the potential energy curves of HF and N<sub>2</sub>, and the singlet–triplet gap of *p*-benzynes with an accuracy similar to that of other multireference perturbation theories.

## Multireference Driven Similarity Renormalization Group


$$\hat{H} \longrightarrow \bar{H}(s) = \hat{U}^\dagger(s) \hat{H} \hat{U}(s) \longrightarrow \bar{H}(\infty)$$

## 1. INTRODUCTION

Multireference (MR) electronic structure theories<sup>1–3</sup> are indispensable tools for accurately describing near-degenerate electronic states. Multireference methods usually separate electron correlation into two contributions:<sup>4</sup> (1) static correlation, which arises from the strong mixing of near-degenerate configurations (determinants), and (2) dynamic correlation, which is associated with small contributions of excited configurations that mostly model the short-range structure of the wave function and dispersion interactions. Static correlation effects can be captured by multideterminantal wave functions.<sup>5–12</sup> However, quantitatively accurate predictions require the simultaneous treatment of static and dynamic electron correlation.

Dynamic correlation effects are commonly introduced via multireference versions of perturbation theory<sup>13–21</sup> (MRPT), configuration interaction (MRCI),<sup>1,22,23</sup> coupled cluster theory (MRCC),<sup>24–32</sup> and other approaches.<sup>33–36</sup> At the core of most multireference theories of dynamic correlation is the similarity transformation of the Hamiltonian ( $\hat{H}$ ) via a wave operator  $\hat{\Omega}$ :

$$\hat{\Omega}: \hat{H} \rightarrow \bar{H} = \hat{\Omega}^{-1} \hat{H} \hat{\Omega} \quad (1)$$

which yields a transformed Hamiltonian  $\bar{H}$ . The purpose of the similarity transformation is to fold a large number of degrees of freedom into the *effective Hamiltonian*, a small part of  $\bar{H}$  that is “decoupled” from the rest of the operator. The effective Hamiltonian describes only a manageable number of states and

can be diagonalized to obtain ground- and excited-state wave functions.

Multireference theories based on effective Hamiltonians are known to suffer from two important problems. The first is the intruder-state problem,<sup>37–39</sup> which is encountered when states that lie within and outside the space spanned by the effective Hamiltonian become near-degenerate. From the perspective of perturbation theory, intruders correspond to excited configurations with vanishing energy denominators. As a consequence, the first-order wave function contains unphysical (often diverging) contributions from excited configurations. The intruder-state problem may be alleviated in MRPT by introducing an empirical level–shift parameter that regularizes the offending denominators.<sup>40,41</sup> For nonperturbative approaches, several techniques have been developed to deal with intruders.<sup>37</sup>

The second difficulty faced by MR effective Hamiltonian theories is the mismatching between the number of wave function parameters and the number of conditions that can be derived from projections of the Schrödinger equation. For instance, state-specific MRCC theories<sup>25–28,42,43</sup> contain redundant wave function parameters, and additional sufficiency conditions must be enforced to ensure a unique solution. Another example is that of internally contracted multireference theories,<sup>44–49</sup> in which excitation operators are linearly

Received: February 10, 2015

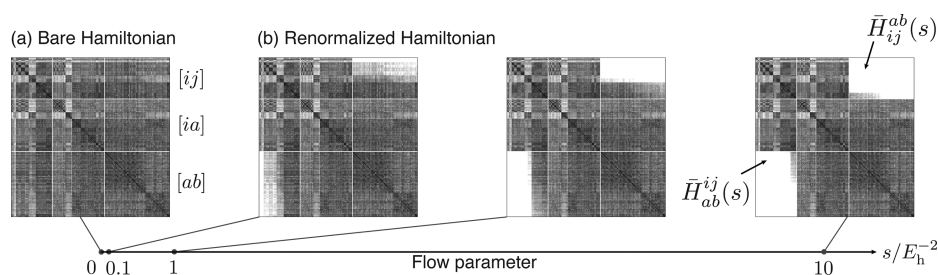


**Figure 1.** Example of the evolution of the two-body components of the transformed Hamiltonian  $[\bar{H}_{pq}^{rs}(s)]$  as a function of the flow parameter  $s$  in the single-reference driven similarity renormalization group.  $\bar{H}_{pq}^{rs}(s)$  is represented as a plot of the matrix  $M_{[pq],[rs]}(s) = \bar{H}_{pq}^{rs}(s)$  where  $[pq]$  and  $[rs]$  are composite indices. The composite indices are divided into three sets: occupied–occupied ( $[ij]$ ), occupied–virtual ( $[ia]$ ), and virtual–virtual ( $[ab]$ ), and the matrix plot shows nine distinct blocks that originate from various combinations of composite indices. For increasing values of  $s$ , the DSRG achieves an increasing decoupling of the block corresponding to  $\bar{H}_{ab}^{ij}(s) = \langle \Phi_{ij}^{ab} | \bar{H}(s) | \Phi \rangle$ , which is responsible for the coupling of the reference ( $\Phi$ ) to doubly excited determinants ( $\Phi_{ij}^{ab}$ ).

dependent and must be orthonormalized. For nonlinear theories, the elimination of linear dependencies introduces numerical instabilities and leads to the appearance of “bumps” in potential energy surfaces.<sup>33,34,36,45,46</sup> One solution to the problem of redundant parametrization is to impose *many-body conditions*. This approach originates in early works of Lindgren<sup>50</sup> and has been used by Nooijen and collaborators to formulate various coupled cluster approaches.<sup>30–32,51</sup>

Electron correlation approaches based on the renormalization group (RG) have recently found interesting applications in quantum chemistry. For example, the density-matrix renormalization group<sup>6–9</sup> (DMRG) has been applied successfully to molecules that are beyond the scope of the traditional complete active space self-consistent field<sup>5</sup> (CASSCF) method.<sup>52–54</sup> In this work we are concerned with a different RG technique introduced recently by one of us: the driven similarity renormalization group (DSRG).<sup>55</sup> The DSRG builds on the similarity renormalization group (SRG), developed independently by Glazek and Wilson<sup>56,57</sup> and Wegner.<sup>58,59</sup> The DSRG is an alternative approach to treat dynamic correlation effects in many-body theories and is based on a series of infinitesimal unitary transformations of the Hamiltonian. The extent of this continuous transformation is controlled by a flow parameter  $s$ , which can be related to an energy cutoff.<sup>55,60,61</sup> Figure 1 illustrates the DSRG transformation of a many-body operator—represented here as a matrix in which the elements are sorted according to the orbital energies. In this example, it can be seen that as the flow parameter increases, the DSRG transformation gradually zeros certain elements of  $\bar{H}(s)$  that couple a closed-shell reference to doubly excited determinants  $[\bar{H}_{ab}^{ij}(s)]$ . As the DSRG transformation progresses, it reduces the elements of  $\bar{H}_{ab}^{ij}(s)$  with large energy denominators and then proceeds to those with small denominators. In this way, if the DSRG transformation is halted at a finite value of  $s$ , it will never attempt to zero the elements of  $\bar{H}_{ab}^{ij}(s)$  with zero energy denominators.

The SRG has found several applications in nuclear physics,<sup>62–64</sup> and in this context it was recently extended to treat open-shell nuclei.<sup>65</sup> However, until recently the only application of the SRG to quantum chemistry consisted of a study of the water molecule by White.<sup>60</sup> In our previous work,<sup>55</sup> the single-reference SRG and DSRG were implemented and benchmarked on ground state equilibrium properties of several diatomic molecules. Our study established that the SRG with one- and two-body operators [SRG(2)] has an accuracy that is intermediate between that of coupled cluster with singles and doubles<sup>66–68</sup> (CCSD) and CCSD with perturbative triples

corrections<sup>69–72</sup> [CCSD(T)]. We also discovered that the SRG cannot easily converge calculations on  $C_2$  and  $F_2$ , and it appears to predict a nonbonded energy minimum for  $F_2$ . These difficulties arise from the fact that the solutions of the SRG approach are found by numerical integration of a set of ordinary differential equations.<sup>55,57,58,60</sup> In certain cases this set of differential equations is ill-conditioned and numerical integration stalls. This problem was the original motivation that lead us to develop the DSRG. In the DSRG, the unitary transformation of the Hamiltonian is parametrized indirectly by a source operator. The source operator can be written in a closed form, and thus, the DSRG equations consist of a set of polynomial equations that can be solved with well established numerical approaches developed for coupled cluster theory. In our benchmark study, the DSRG was shown to yield results that are similar to those obtained from the SRG. In addition, we found no instance in which the DSRG equations fail to converge or yields anomalous results.

The goal of this work is to extend the DSRG approach to a general multireference wave function. In order to explore the pivotal properties of the multireference DSRG (MR-DSRG) theory, we conduct a perturbative analysis of the corresponding equations at second order. The resulting DSRG second-order multireference perturbation theory (DSRG-MRPT2) has several attractive features: (1) it is size extensive, (2) it can be evaluated in a noniterative fashion, and (3) it demands at most a three-particle density cumulant.<sup>73–77</sup> We will start by formulating the general DSRG approach based on a multireference wave function in section 2.2, where the generalized normal ordered operators<sup>73,78,79</sup> and many-body conditions<sup>30,50,51</sup> are employed. In section 2.3, we derive the DSRG-MRPT2 equations. What follows is a discussion of the formal properties of the MR-DSRG in sections 2.4 and 2.5. In section 3, we apply the DSRG-MRPT2 to compute the dissociation curves of hydrogen fluoride and nitrogen molecules, along with their spectroscopic constants, and the singlet–triplet separation of the *p*-benzynes molecule. Finally, in section 4 we will discuss our findings and propose future extensions of the MR-DSRG theory.

## 2. THEORY

**2.1. Synopsis of the DSRG Theory.** In the unitary DSRG formalism,<sup>55</sup> the bare Hamiltonian ( $\hat{H}$ ) is brought to a diagonal form by a continuous unitary transformation:

$$\hat{H} \rightarrow \bar{H}(s) = \hat{U}^\dagger(s) \hat{H} \hat{U}(s) \quad (2)$$

where  $\bar{H}(s)$  is the transformed Hamiltonian and  $\hat{U}(s)$  is a unitary operator that depends on a time-like parameter  $s$  defined in the range  $[0, \infty)$ . At the beginning of the transformation ( $s = 0$ ) we require that  $\hat{U}(0) = \hat{1}$  so that the DSRG Hamiltonian coincides with the bare Hamiltonian. In the limit of  $s \rightarrow \infty$  we instead require that the unitary transformation exactly decouples the reference from excited states.

The unitary DSRG<sup>55</sup> postulates that the flow of the Hamiltonian is driven by an Hermitian  $s$ -dependent source operator  $\hat{R}(s)$ . More specifically, the nondiagonal part of the transformed Hamiltonian,  $[\bar{H}(s)]_N$ , is equal to the source operator for all values of  $s$ :

$$[\bar{H}(s)]_N = \hat{R}(s) \quad (3)$$

Therefore, once the source operator is specified, the DSRG equation [eq 3] implicitly defines the unitary transformation  $\hat{U}(s)$ . The nondiagonal part of  $\bar{H}(s)$  contains those Hugenholtz diagrams closed from the bottom and from the top, which correspond to pure excitation and de-excitation components of the Hamiltonian, respectively.<sup>80,81</sup> The electronic energy is obtained by taking the expectation value of the transformed Hamiltonian:

$$E(s) = \langle \Phi | \bar{H}(s) | \Phi \rangle \quad (4)$$

It is important to notice that the DSRG equation [eq 3] and the energy [eq 4] are evaluated at fixed values of the flow parameter and do not require numerical integration such as in the case of the SRG.

**2.2. Formulation of the DSRG Based on a Generalized Reference Wave Function.** In this section, we will formulate a unitary version of the DSRG using the formalism of generalized normal ordering.<sup>73,78,79,82,83</sup> For a detailed introduction to the generalized normal ordering we direct the reader to refs 42, 73, 78, 79, 82, and 83. Additionally, we provide a summary of this topic in the Supporting Information. Following the conventional definition of active space, the spin orbitals  $\{\phi^p, p = 1, \dots, N\}$  are partitioned into three distinct subsets: core (C), active (A), and virtual (V), of dimensions  $N_C$ ,  $N_A$ , and  $N_V$ , respectively. For convenience, we also consider the sets of generalized hole (H) and particle (P) spin orbitals, defined as  $\mathbf{H} = \mathbf{C} \cup \mathbf{A}$  and  $\mathbf{P} = \mathbf{A} \cup \mathbf{V}$ , of size  $N_H$  and  $N_P$ , respectively. Figure 2 summarizes the orbital spaces and the corresponding orbital index notation used in this work.

The generalized Fermi vacuum  $\Phi$  used to define the operator normal ordering is a linear combination of Slater determinants  $(\Phi_\mu)$  weighted by the coefficients  $\{c_\mu\}$ ,

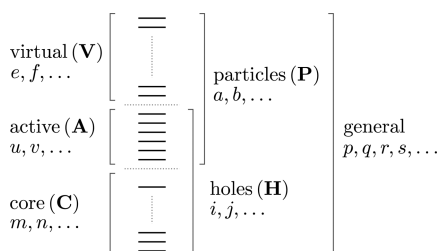


**Figure 2.** Definition of orbital spaces and their corresponding orbital indices used in this work.

$$|\Phi\rangle = \sum_{\mu=1}^d c_\mu |\Phi_\mu\rangle \quad (5)$$

where, without loss of generality,  $|\Phi\rangle$  is normalized to one. The determinants that enter in the definition of  $\Phi$  are chosen to form a complete active space of dimension  $d$ ,  $M_0 = \{|\Phi_\mu\rangle, \mu = 1, \dots, d\}$ . That is, we consider all determinants  $\Phi_\mu$  with occupied core orbitals and a given number of active electrons ( $n_{\text{act}}$ ) distributed in the active orbitals:

$$|\Phi_\mu\rangle = \underbrace{\hat{a}^u \hat{a}^v \dots}_{n_{\text{act}}} \prod_m^C \hat{a}^m | \rangle \quad (6)$$

where  $| \rangle$  is the true vacuum and  $\hat{a}^p$  ( $\hat{a}_p$ ) is a second quantized creation (annihilation) operator.

The second-quantized bare Hamiltonian written in the normal ordered form with respect to the vacuum  $\Phi$  is

$$\hat{H} = E_0 + \sum_{pq} f_p^q \{\hat{a}_q^p\} + \frac{1}{4} \sum_{pqrs} v_{pq}^{rs} \{\hat{a}_{rs}^{pq}\} \quad (7)$$

where  $E_0 = \langle \Phi | \hat{H} | \Phi \rangle$  is the energy of the reference  $\Phi$  and  $f_p^q$  is the matrix element of the generalized Fock matrix. The latter is computed from the standard one-electron integrals ( $h_p^q = \langle \phi_q | \hat{h} | \phi_p \rangle$ ), the antisymmetrized two-electron integrals ( $v_{rs}^{pq} = \langle \phi_p \phi_s | \phi^p \phi^q \rangle$ ), and the one-particle density matrix of the reference ( $\gamma_q^p = \langle \Phi | \hat{a}^p \hat{a}_q | \Phi \rangle$ ):

$$f_p^q = h_p^q + \sum_{rs} v_{pr}^{qs} \gamma_s^r \quad (8)$$

In eq 7, the creation and annihilation operators are written in a compact form,

$$\hat{a}_{ij\dots}^{ab\dots} = \hat{a}^a \hat{a}^b \dots \hat{a}_i \hat{a}_j \quad (9)$$

and normal ordering of the operators is indicated by curly braces.

The DSRG transformed Hamiltonian  $\bar{H}(s)$  may be expressed in the normal ordered form with respect to  $\Phi$  and in general it will be the sum of a scalar term  $[\bar{H}_0(s)]$  and various  $k$ -body operators  $[\bar{H}_k(s)]$  with rank  $k$  as high as the total number of electrons:<sup>30,55</sup>

$$\bar{H}(s) = \bar{H}_0(s) + \bar{H}_1(s) + \bar{H}_2(s) + \bar{H}_3(s) + \dots \quad (10)$$

where a generic  $k$ -body operator  $\bar{H}_k(s)$  is defined as

$$\bar{H}_k(s) = \frac{1}{(k!)^2} \sum_{pqrs\dots} \bar{H}_{pq\dots}^{rs\dots}(s) \{\hat{a}_{rs\dots}^{pq\dots}\} \quad (11)$$

The unitary operator  $\hat{U}(s)$  is conveniently parametrized as the exponential of an anti-Hermitian operator  $\hat{A}(s)$ :

$$\hat{U}(s) = e^{\hat{A}(s)} \quad (12)$$

where  $\hat{A}(s)$  is truncated to a given substitution level  $n$ :

$$\hat{A}(s) = \sum_{k=1}^n \hat{A}_k(s) \quad (13)$$

Each  $k$ -body component of  $\hat{A}(s)$   $[\hat{A}_k(s)]$  is related to an excitation operator  $[\hat{T}_k(s)]$ :

$$\hat{A}_k(s) = \hat{T}_k(s) - \hat{T}_k^\dagger(s) \quad (14)$$

$$\hat{T}_k(s) = \frac{1}{(k!)^2} \sum_{ij\dots}^H \sum_{ab\dots}^P t_{ab\dots}^{ij\dots}(s) \{\hat{a}_{ij\dots}^{ab\dots}\} \quad (15)$$

The cluster amplitudes  $[t_{ab\dots}^{ij\dots}(s)]$  are tensors antisymmetric with respect to the individual permutation of upper and lower indices. In the definition of  $\hat{T}_k$ , internal amplitudes corresponding to substitutions involving only active spin orbitals are excluded,

$$t_{uv\dots}^{xy\dots} = 0, \quad u, v, x, y \in \mathbf{A} \quad (16)$$

since their effect is to relax the coefficients that define the reference wave function ( $c_\mu$ ).

The source operator  $[\hat{R}(s)]$  contains contributions from normal ordered many-body operators of different rank:

$$\hat{R}(s) = \hat{R}_1(s) + \hat{R}_2(s) + \dots \quad (17)$$

There is no scalar contribution in eq 17 since  $\hat{R}(s)$  contains only excitation and de-excitation operators. In accordance with the boundary conditions imposed onto  $\hat{U}(s)$ , we impose the following requirements onto  $\hat{R}(s)$ : (1) when  $s = 0$ , the nondiagonal component of  $\bar{H}$  is identical to the bare Hamiltonian,

$$\hat{R}(0) = [\bar{H}(0)]_N = \hat{H}_N \quad (18)$$

and (2) when  $s \rightarrow \infty$ , the nondiagonal elements of the Hamiltonian vanish,

$$\hat{R}(\infty) = [\bar{H}(\infty)]_N = 0 \quad (19)$$

So far, we have not explicitly identified the expressions for the source operator. For  $\hat{R}_k(s)$ , we adopt the same parametrization as our previous work, which is determined from a perturbative analysis of the single-reference SRG equations,<sup>55</sup>

$$r_{ab\dots}^{ij\dots}(s) = [\bar{H}_{ab\dots}^{ij\dots}(s) + t_{ab\dots}^{ij\dots}(s) \Delta_{ab\dots}^{ij\dots}] e^{-s(\Delta_{ab\dots}^{ij\dots})^2} \quad (20)$$

and  $r_{ij\dots}^{ab\dots}(s) = [r_{ab\dots}^{ij\dots}(s)]^*$ . In eq 20  $\Delta_{ab\dots}^{ij\dots}$  is a generalized Møller–Plesset denominator defined in terms of the diagonal components of the Fock matrix ( $\varepsilon_p = f_p^p$ ),

$$\Delta_{ab\dots}^{ij\dots} = \varepsilon_i + \varepsilon_j + \dots - \varepsilon_a - \varepsilon_b - \dots \quad (21)$$

Equations 2–4 and 10–20 define our unitary multireference DSRG approach. Notice that the DSRG flow equation [eq 3] is a set of *many-body* conditions, and it should be interpreted as equating the various normal ordered operator components of  $[\bar{H}(s)]_N$  and  $\hat{R}(s)$ . When the left-hand side of the DSRG flow equation [eq 3] is expanded using the Baker–Campbell–Hausdorff (BCH) formula and the operator components are equated to that of the source operator, one obtains a set of polynomial equations in the amplitudes  $t_{ab\dots}^{ij\dots}(s)$ . In the unitary version of the DSRG, these equations do not truncate, so practical implementations have to resort to use an approximated BCH formula.<sup>33,84</sup> Alternatively, it is possible to formulate a coupled cluster version of the multireference DSRG, in which the unitary transformation is replaced by a similarity transformation carried out by the exponential of an excitation operator. Nevertheless, these considerations do not affect the perturbative analysis of the DSRG equations carried out in this work. It is also not obvious that the MR-DSRG equations based on the source operator given in eq 20 always have a solution. However, our previous work<sup>55</sup> on the single-reference DSRG showed that solutions of the *nonperturbative* equations can be found even in challenging cases. For example,

the dissociation curve of H<sub>2</sub>O was computed with the single-reference DSRG without encountering convergence problems.

The source operator can be used to illustrate some of the features of the DSRG approach. In both the SRG and the DSRG, the time-like parameter  $s$  has a unit of [energy]<sup>−2</sup> and can be associated with an energy cutoff defined as  $\Lambda = s^{-1/2}$ .<sup>55,61</sup> The many-body components of  $\bar{H}$  that couple the reference  $|\Phi\rangle$  to internally contracted excited configurations  $\hat{a}_{ij\dots}^{ab\dots}|\Phi\rangle$  can be identified with the matrix elements  $\bar{H}_{ab\dots}^{ij\dots}(s)$ . For a fixed value of  $s$ , the elements of  $\bar{H}_{ab\dots}^{ij\dots}(s)$  with  $|\Delta_{ab\dots}^{ij\dots}|$  larger than  $\Lambda$  are approximately zero. On the contrary, if  $|\Delta_{ab\dots}^{ij\dots}| \ll \Lambda$ , then the corresponding  $\bar{H}_{ab\dots}^{ij\dots}(s)$  is in general nonzero. Thus, in the DSRG (and SRG) the parameter  $s$  can be used to separate different energy scales of the Hamiltonian, which are expressed as the energy difference between the reference and its excitations or de-excitations. The partial decoupling of the Hamiltonian achieved by the DSRG sets this formalism apart from other nonperturbative many-body approaches. Moreover, this feature is also what guarantees the avoidance of the intruder-state problem in multireference many-body approaches based on the DSRG. This aspect is investigated further in sections 2.4 and 3.3.

### 2.3. Perturbative Analysis of the MR-DSRG Equations.

Some of the features of the MR-DSRG theory can be appreciated by conducting a perturbative analysis of the corresponding equations. We will restrict this study to the case of a fixed reference; that is, we ignore the relaxation of the coefficients  $c_\mu$  that enter the definition of  $|\Phi\rangle$  in eq 5. Our analysis begins by partitioning the bare Hamiltonian [eq 7] into a zeroth-order term  $\hat{H}^{(0)}$  plus a first-order perturbation  $\hat{H}^{(1)}$  dependent on the parameter  $\xi$ ,

$$\hat{H} = \hat{H}^{(0)} + \xi \hat{H}^{(1)} \quad (22)$$

The zero-order Hamiltonian includes the reference energy ( $E_0$ ) and a one-body operator  $[\hat{F}^{(0)}]$ ,

$$\hat{H}^{(0)} = E_0 + \hat{F}^{(0)} \quad (23)$$

where  $\hat{F}^{(0)}$  contains the diagonal blocks of the Fock matrix corresponding to the core, active, and virtual orbitals:

$$\hat{F}^{(0)} = \sum_{mn}^C f_m^n \{\hat{a}_n^m\} + \sum_{uv}^A f_u^v \{\hat{a}_v^u\} + \sum_{ef}^V f_e^f \{\hat{a}_f^e\} \quad (24)$$

This choice of  $\hat{F}^{(0)}$  guarantees that  $\hat{H}^{(0)}$  is invariant with respect to separate rotations of core, active, and virtual orbitals. To simplify the structure of  $\hat{F}^{(0)}$ , we work in the basis of semicanonical orbitals, defined in such a way that the core, active, and virtual blocks of the generalized Fock matrix are diagonal.<sup>85,86</sup> Thus, the zeroth-order generalized Fock operator is simply

$$\hat{F}^{(0)} = \sum_p \varepsilon_p \{\hat{a}_p^p\} \quad (25)$$

and it can be expressed using only a set of orbital energies  $\{\varepsilon_p\}$ , which are the diagonal elements of the generalized Fock matrix,  $\varepsilon_p = f_p^p$ . The resulting first-order Hamiltonian then contains the one- and two-body terms  $\hat{F}^{(1)}$  and  $\hat{V}^{(1)}$ ,

$$\hat{H}^{(1)} = \hat{H} - \hat{H}^{(0)} = \hat{F}^{(1)} + \hat{V}^{(1)} \quad (26)$$

where the one-body operator  $\hat{F}^{(1)}$  involves only the off-diagonal contributions (e.g., coupling orbitals in C and V, etc.) and the



two-body operator  $\hat{V}^{(1)}$  corresponds to the full two-body operator  $\hat{V} = (1/4) \sum_{pqrs} v_{pq}^{rs} \{\hat{a}_{rs}^{pq}\}$ .

The perturbation theory derived from the many-body formulation of MR-DSRG is obtained by writing the DSRG energy and flow equations [eqs 3 and 4] as depending on the perturbation ordering parameter  $\xi$ :

$$E(s, \xi) = \langle \Phi | \bar{H}(s, \xi) | \Phi \rangle \quad (27)$$

$$\hat{R}(s, \xi) = [\bar{H}(s, \xi)]_N = [e^{-\hat{A}(s, \xi)} \hat{H} e^{\hat{A}(s, \xi)}]_N \quad (28)$$

where the source operator  $[\hat{R}(s, \xi)]$ , the anti-Hermitian operator  $[\hat{A}(s, \xi)]$ , and the energy  $[E(s, \xi)]$  are expanded in power series of  $\xi$ :

$$\hat{R}(s, \xi) = \hat{R}^{(0)}(s) + \xi \hat{R}^{(1)}(s) + \xi^2 \hat{R}^{(2)}(s) + \dots \quad (29)$$

$$\hat{A}(s, \xi) = \hat{A}^{(0)}(s) + \xi \hat{A}^{(1)}(s) + \xi^2 \hat{A}^{(2)}(s) + \dots \quad (30)$$

$$E(s, \xi) = E^{(0)}(s) + \xi E^{(1)}(s) + \xi^2 E^{(2)}(s) + \dots \quad (31)$$

Expanding the transformed Hamiltonian  $[\bar{H}(s, \xi)]$  and subsequently collecting terms with the same power of  $\xi$  yields the working equations for the MR-DSRG perturbation theory.

The zeroth-order DSRG equation is satisfied by the trivial solution  $\hat{A}^{(0)}(s) = 0$ , which implies that zero-order energy corresponds to the energy of the reference,

$$E^{(0)}(s) = \langle \Phi | \bar{H}^{(0)}(s) | \Phi \rangle = \langle \Phi | E_0 + \hat{F}^{(0)} | \Phi \rangle = E_0 \quad (32)$$

where we have employed the fact that  $\hat{F}^{(0)}$  is normal ordered with respect to the vacuum  $\Phi$ .

The first-order contribution to the energy is null,

$$E^{(1)}(s) = \langle \Phi | \hat{H}^{(1)} + [\hat{H}^{(0)}, \hat{A}^{(1)}(s)] | \Phi \rangle = 0 \quad (33)$$

since  $\hat{H}^{(1)}$  is normal ordered with respect to  $\Phi$  and  $\hat{A}^{(1)}(s)$  does not contain internal excitations. The first-order DSRG equation

$$\hat{R}^{(1)}(s) = [\bar{H}^{(1)}(s)]_N = (\hat{H}^{(1)} + [\hat{H}^{(0)}, \hat{A}^{(1)}(s)])_N \quad (34)$$

leads to the following expressions for the first-order amplitudes:

$$t_a^{i,(1)}(s) = \frac{[f_a^{i,(1)} + \sum_{ux} \Delta_{ux}^x t_{ax}^{iu,(1)}(s) \gamma_u^x] [1 - e^{-s(\Delta_a^i)^2}]}{\epsilon_i - \epsilon_a} \quad (35)$$

$$t_{ab}^{ij,(1)}(s) = \frac{v_{ab}^{ij,(1)} [1 - e^{-s(\Delta_{ab}^{ij})^2}]}{\epsilon_i + \epsilon_j - \epsilon_a - \epsilon_b} \quad (36)$$

Notice that when  $|\Delta_{ab}^{ij}|$  (or  $|\Delta_a^i|$ ) is greater than the energy cutoff  $\Lambda = s^{-1/2}$ , the first-order amplitudes resemble the equations of open-shell perturbation theory. Equations 35 and 36 were derived using the generalized Wick's theorem, and details are provided in the Supporting Information.

The first nontrivial correction to the energy appears at second order with respect to the perturbation parameter  $\xi$ ,

$$\begin{aligned} E^{(2)}(s) &= \langle \Phi | [\hat{H}^{(1)}, \hat{A}^{(1)}(s)] | \Phi \rangle \\ &\quad + \frac{1}{2} \langle \Phi | [[\hat{H}^{(0)}, \hat{A}^{(1)}(s)], \hat{A}^{(1)}(s)] | \Phi \rangle \\ &= \frac{1}{2} \langle \Phi | [\bar{H}^{(1)}(s), \hat{A}^{(1)}(s)] | \Phi \rangle \end{aligned} \quad (37)$$

where we used eq 34 to simplify the energy expression and introduced a modified first-order effective Hamiltonian,  $\tilde{H}^{(1)}(s) = \hat{H}^{(1)}(s) + \hat{R}^{(1)}(s)$ , with  $s$ -dependent nondiagonal components:

$$\tilde{f}_a^{i,(1)}(s) = f_a^{i,(1)} [1 + e^{-s(\Delta_a^i)^2}] + [\sum_{ux} \Delta_{ux}^x t_{ax}^{iu,(1)}(s) \gamma_u^x] e^{-s(\Delta_a^i)^2} \quad (38)$$

$$\tilde{v}_{ab}^{ij,(1)}(s) = v_{ab}^{ij,(1)} [1 + e^{-s(\Delta_{ab}^{ij})^2}] \quad (39)$$

The various terms that contribute to the DSRG-MRPT2 energy are reported in Table 1. These energy contributions are given in

**Table 1. DSRG-MRPT2 Zeroth- and Second-Order Energy Expressions<sup>a</sup>**

term	energy expression
$E^{(0)}$	$f_p^q \gamma_q^p - (1/2) v_{pq}^{rs} \gamma_r^p \gamma_s^q + (1/4) v_{pq}^{rs} \lambda_{rs}^{pq}$
$(1/2) \langle [\tilde{H}^{(1)}(s), \hat{A}_1^{(1)}(s)] \rangle$	$+ \tilde{f}_j^{b,(1)}(s) t_a^{i,(1)}(s) \gamma_i^a \eta_{ab}^b$
$(1/2) \langle [\tilde{V}^{(1)}(s), \hat{A}_1^{(1)}(s)] \rangle$	$+ (1/2) \tilde{v}_{xy}^{uv,(1)}(s) t_x^{\mu,(1)}(s) \lambda_{uv}^{xy} - (1/2) \tilde{v}_{my}^{nu,(1)}(s) t_x^m(s) \lambda_{uv}^{xy}$
$(1/2) \langle [\tilde{H}^{(1)}(s), \hat{A}_2^{(1)}(s)] \rangle$	$+ (1/2) \tilde{f}_x^{e,(1)}(s) t_{xy}^{\mu\nu,(1)}(s) \lambda_{uv}^{xy} - (1/2) \tilde{f}_m^{v,(1)}(s) t_{xy}^{\mu\nu,(1)}(s) \lambda_{uv}^{xy}$
$(1/2) \langle [\tilde{V}^{(1)}(s), \hat{A}_2^{(1)}(s)] \rangle$	$+ (1/4) \tilde{v}_{kl}^{cd,(1)}(s) t_{ab}^{ij,(1)}(s) \gamma_i^k \gamma_j^l \eta_{cd}^{ab} + (1/8) \tilde{v}_{xy}^{cd,(1)}(s) t_{ab}^{\mu\nu,(1)}(s) \eta_{cd}^{ab} \lambda_{uv}^{xy} + (1/8) \tilde{v}_{kl}^{mn,(1)}(s) t_{xy}^{ij,(1)}(s) \gamma_i^k \gamma_j^l \lambda_{uv}^{xy} + \tilde{v}_{jk}^{ib,(1)}(s) t_{xy}^{\mu\nu,(1)}(s) \gamma_i^a \eta_{ab}^b \lambda_{uv}^{xy} + (1/4) \tilde{v}_{iz}^{\mu\nu,(1)}(s) t_{xy}^{\mu\nu,(1)}(s) \lambda_{uv}^{xyz} + (1/4) \tilde{v}_{xy}^{wa,(1)}(s) t_{az}^{\mu\nu,(1)}(s) \lambda_{uv}^{xyz}$

<sup>a</sup>All quantities are given in terms of the one-particle density matrix ( $\gamma_q^p$ ), the one-hole density matrix ( $\eta_q^p$ ), the two-body cumulant ( $\lambda_{xy}^{uv}$ ), and the three-body cumulant ( $\lambda_{xyz}^{uvw}$ ) of the reference ( $\Phi$ ). The Einstein convention for the summation over the repeated indices is employed. See Figure 2 for the definition of the orbital spaces and their corresponding indices.

terms of the modified one- and two-body integrals  $[\tilde{f}_a^{i,(1)}(s)$  and  $\tilde{v}_{ab}^{ij,(1)}(s)]$ , the one-particle density matrix ( $\gamma$ ), the one-hole density matrix defined as the difference between identity matrix and one-particle density matrix ( $\eta = 1 - \gamma$ ), and the two- and three-body cumulants ( $\lambda_2, \lambda_3$ ) of the reference wave function.

The first-order amplitude equations [eqs 35 and 36] together with the expressions for the second-order energy [eq 37 and Table 1] define the second-order MR-DSRG perturbation theory (DSRG-MRPT2). It is worth pointing out several advantages of the DSRG-MRPT2 method. The first-order amplitudes and  $E^{(2)}$  can be computed via an efficient noniterative procedure that, in most common situations ( $N_A \ll N_C < N_V$ ) and excluding the cost of the integral transformation, is dominated by a term proportional to  $O(N_H^2 N_P^2)$ . Although our formulation of the DSRG-MRPT2 requires at most the three-particle density cumulant ( $\lambda_3$ ), resulting in a  $O(N_A^6 N_V)$  scaling with respect to the number of active orbitals, this is not expected to be a major bottleneck when  $N_A < 20-30$ . However, we also consider an approximate version of the DSRG-MRPT2 in which the three-body cumulant is neglected from the  $E^{(2)}$  equations. This approximation avoids the  $O(N_A^6)$  memory cost required to store  $\lambda_3$  and reduces the scaling of  $E^{(2)}$  with respect to the

number of active orbitals down to  $O(N_A^4 N_V^2)$ . Also notice that a novel renormalization term  $[\hat{R}^{(1)}(s)]$  appears in the expression of  $E^{(2)}$ . In our numerical studies we found that, for finite values of  $s$ ,  $\hat{R}^{(1)}(s)$  has the net effect of increasing the magnitude of the second-order correlation energy. As  $s \rightarrow \infty$ , the energy contribution from  $\hat{R}^{(1)}(s)$  gradually vanishes.

We end this section by pointing out connections between the  $s \rightarrow \infty$  limit of the DSRG-MRPT2 and other perturbation theories. In the general case, DSRG-MRPT2 ( $s \rightarrow \infty$ ) is analogous to Brandow's second-order multireference many-body perturbation theory (MR-MBPT2),<sup>87</sup> with the difference being that in the former case the reference is a multi-determinantal wave function instead of a core closed-shell determinant. When the model space consists of a single high-spin open-shell determinant, the DSRG-MRPT2 ( $s \rightarrow \infty$ ) reproduces the second-order restricted open-shell Møller–Plesset (ROMP) theory of Amos et al.,<sup>88</sup> while in the case of a single closed-shell determinant, the DSRG-MRPT2 ( $s \rightarrow \infty$ ) is identical to the second-order Møller–Plesset (MP2) energy.

**2.4. Avoidance of Intruders in the DSRG.** An analysis of the amplitude expressions of eqs 35 and 36 in the limit of small energy denominators elucidates the mechanism by which the MR-DSRG avoids the intruder-state problem. For example, as  $|\Delta_{ab}^{ij}| \rightarrow 0$ , the  $t_{ab}^{ij(1)}(s)$  amplitude can be expressed as a Taylor series of  $f(z) = (1 - e^{-z})/z$  expanded in the dimensionless variable  $z = (s)^{1/2} \Delta_{ab}^{ij}$ :

$$t_{ab}^{ij(1)}(s) = v_{ab}^{ij(1)} \sqrt{s} f(z) = s v_{ab}^{ij(1)} \Delta_{ab}^{ij} + O[s^{3/2} (\Delta_{ab}^{ij})^3] \quad (40)$$

and similarly for the  $t_1$  amplitude equation. Equation 40 shows that for finite values of  $s$ , small energy denominators cannot cause the DSRG-MRPT2 first-order amplitudes to diverge. As a consequence,  $E^{(2)}(s)$  is also well behaved when one or more energy denominators approach or become equal to zero. This feature of the DSRG-MRPT2 is due to the term  $f(z)$  in eq 40, which may be viewed as a subtle way to regularize the energy denominators. We also notice that the function  $f(z)$  is odd with respect to  $z$  and goes to zero as  $z \rightarrow 0$ . For a fixed value of  $v_{ab}^{ij(1)}$  when the energy denominator  $\Delta_{ab}^{ij}$  goes from zero to infinity,  $t_{ab}^{ij(1)}(s)$  first increases and then decreases. As a consequence, the DSRG regularization may introduce “ripples” in potential energy surfaces. However, this problem cannot be avoided because any odd regularization function that yields a finite amplitude in the limit  $\Delta_{ab}^{ij} \rightarrow 0$  will have a discontinuity at the origin and—even worse—will introduce “jumps” in potential energy surfaces. This happens, for example, if the regularized denominator takes the form  $g(z) = (1 - e^{-|z|})/z$ .

Both the perturbative and nonperturbative versions of the DSRG (and the SRG) are inherently intruder free, and this feature differentiates them from regularization techniques commonly applied *a posteriori* to address the intruder-state problem in multireference perturbation theories.<sup>40,41,89</sup> The DSRG-MRPT2 regularized denominator may also be related to the restrained denominator MP2 of Ohnishi et al.,<sup>90</sup> which has been employed to improve the accuracy of intermolecular interaction energies computed with MP2. This approach uses a modified denominator of the form  $\max(\tau, \Delta_{ab}^{ij})$ , where  $\tau$  is an energy threshold set equal to approximately  $2.4 E_h$ . Interestingly, this energy threshold falls within the optimal range of energy cutoff identified in this work ( $\Lambda \in [1, 3] E_h$ ).

How should one choose the flow parameter  $s$  in the DSRG-MRPT2 approach? This question will be addressed in two

ways. Here we provide boundaries on  $s$  that are deduced by imposing conditions on the DSRG transformation, while in section 3.3 we study how the choice of  $s$  affects the accuracy of the DSRG-MRPT2 energy. In general, the choice of  $s$  is dictated by two requirements. On one hand, the amount of correlation energy recovered by the DSRG increases with  $s$ , so this quantity should be chosen to be as large as possible. On the other hand, if  $s$  is too large, the DSRG will be more sensitive to small energy denominators. Our objective is to determine an upper bound on  $s$  that guarantees that the DSRG transformation avoids the appearance of intruder states, corresponding to large  $t$  amplitudes. To this end, we seek a condition on  $s$  to ensure that the absolute value of the DSRG amplitudes is less than a certain maximum value ( $t_{\max}$ ):

$$\|t_{ab}^{ij(1)}(s)\|_{\max} < t_{\max} \quad (41)$$

where  $\|\cdot\|_{\max}$  indicates the elementwise maximum norm of a tensor. To impose eq 41, we first notice that the following inequality holds:

$$\|t_{ab}^{ij(1)}(s)\|_{\max} \leq \|v_{ab}^{ij(1)}\|_{\max} \max_z |f(z)| \sqrt{s} \quad (42)$$

A sufficiency condition that satisfies eq 41 can be derived by imposing:

$$\|v_{ab}^{ij(1)}\|_{\max} \max_z |f(z)| \sqrt{s} < t_{\max} \quad (43)$$

Using the fact that the maximum of  $|f(z)|$  with respect to  $z$  is  $\max_z |f(z)| = (1 - e^{-c})/c = 0.6382$ , where  $c = 1.1209$ , we arrive at the following condition:

$$s < \left[ \frac{t_{\max}}{0.6382 \|v_{ab}^{ij(1)}\|_{\max}} \right]^2 \quad (44)$$

Equation 44 can be used to derive an upper bound for  $s$ . A reasonable choice of  $t_{\max}$  is 0.1, which is equivalent to requiring that no excited configuration has a weight larger than 1%. Furthermore, we assume that the maximum value of two-electron integral for valence–valence excitations is around  $0.1 E_h$  ( $\|v_{ab}^{ij(1)}\|_{\max} \approx 0.1$ ). Under these assumptions we obtain the condition  $s < 2.46 E_h^{-2}$ , which is equivalent to an energy cutoff  $\Lambda > 0.64 E_h$ . We take this result as an indication that  $s$  should be chosen to be of the order of one  $E_h^{-2}$  or less.

**2.5. Formal Aspects of the MR-DSRG.** In this section we discuss formal properties of the MR-DSRG, including the invariance of the energy with respect to orbital rotations, size consistency and extensivity, and vacuum relaxation effects. The source operator used in this work [eq 20] is identical to the one previously used in the single-reference DSRG,<sup>55</sup> and it is not orbital invariant. However, we have recently discovered that it is possible to write a more general version of the source operator that is orbital invariant and that coincides with eq 20 in a semicanonical orbital basis. Since in the DSRG-MRPT2 it is always computationally advantageous to work with a diagonal zeroth-order operator, the issue of restoring orbital invariance has little practical importance. Therefore, we leave this topic for future work on nonperturbative versions of the MR-DSRG.

Since all quantities that enter the MR-DSRG energy and amplitude equations are connected, this theory and the DSRG-MRPT2 are size extensive. The connectivity of the MR-DSRG equations also implies that if the molecular orbital basis is

localized on separate molecular fragments, then the sum of the energy of isolated fragments is equal to the energy computed on a supramolecular species composed of noninteracting fragments.<sup>91</sup> Size consistency was confirmed numerically on the systems  $\text{H}_2 \cdots \text{H}_2$  and  $\text{HF} \cdots \text{HF}$  using a four-electron in four-orbital active space for the supramolecular species and a two-electron in two-orbital active space for the individual fragments.

Finally, we comment on the issue of relaxation of the reference in the MR-DSRG and other multireference theories based on generalized normal ordering. Any formalism that expresses the exact wave function ( $|\Psi\rangle$ ) as a wave operator  $\hat{\Omega}$  applied to a multideterminantal reference,  $|\Psi\rangle = \hat{\Omega}|\Phi\rangle$ , must either allow the reference to relax by treating the expansion coefficients as variables, or include internal amplitudes that can change the weight of the reference determinants in  $\hat{\Omega}$ . The first option is usually the most convenient, and it produces theories that are numerically robust. For example, this approach is at the basis of recent formulations of the internally contracted multireference theories.<sup>45–49,92</sup> Reference relaxation effects can be introduced in the MR-DSRG following the same approach used in other internally contracted multireference theories. In practice this requires solving the MR-DSRG equations and diagonalizing  $\bar{H}$  in the model space until a self-consistent solution is reached. As the reference changes, so do the density matrix, the cumulants, and the normal ordered operators. Alternatively, the DSRG transformed Hamiltonian can be diagonalized in a space of determinants (configurations)—generally much larger than the model space—that accounts for orbital and reference relaxation. This strategy is followed for example in several multireference coupled cluster methods developed by Nooijen and co-workers.<sup>29–32</sup>

### 3. RESULTS

**3.1. Dissociations of Hydrogen Fluoride and Nitrogen.** The accuracy of DSRG-MRPT2 was initially tested on the potential energy curves of the  $X^1\Sigma^+$  state of hydrogen fluoride and the  $X^1\Sigma_g^+$  state of the nitrogen molecule. A two-electron two-orbital CASSCF [CASSCF(2,2)] reference was employed for HF, while a six-electron in six-orbital CASSCF [CASSCF(6,6)] reference was used for  $\text{N}_2$ . Comparisons with second-order complete-active-space perturbation theory (CASPT2),<sup>13,14,93</sup> the partially contracted variant of second-order  $n$ -electron valence perturbation theory (pc-NEVPT2),<sup>17–20</sup> Mukherjee second-order perturbation theory (Mk-MRPT2),<sup>25,26,42,43,94</sup> internally contracted multireference configuration interaction with singles and doubles<sup>22,23</sup> and Davidson's correction<sup>95</sup> (ic-MRCISD+Q), and full configuration interaction (FCI) were made where possible. All computations employed Dunning's correlation-consistent cc-pVDZ basis set.<sup>96</sup> The 1s-like CASSCF molecular orbitals on nitrogen and fluorine atoms were excluded from the correlation treatment. The DSRG-MRPT2 method was implemented as a plugin to the Psi4<sup>97</sup> package. CASSCF,<sup>98,99</sup> CASPT2, pc-NEVPT2, ic-MRCISD+Q, and FCI results were obtained using the Molpro 2010.1 package,<sup>100</sup> while Mk-MRPT2 energies were computed with Psi4.<sup>97</sup>

The potential energy curves (PECs) for the lowest singlet state of HF and  $\text{N}_2$  are depicted in the upper panel of Figures 3 and 4, respectively. In the case of  $\text{N}_2$ , we use ic-MRCISD+Q as the benchmark since it is more affordable and is known to provide highly parallel results compared to FCI.<sup>23,102</sup> As illustrated in Figure 4, ic-MRCISD+Q (the black curve) deviates from FCI results<sup>101</sup> (gray dots) by at most 1.8 mE<sub>h</sub>

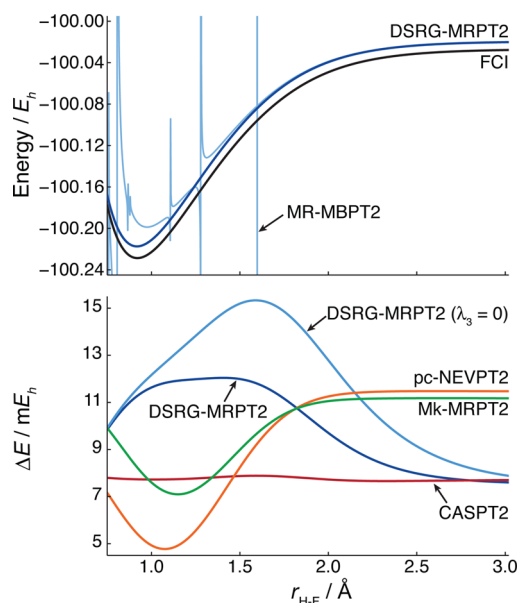


**Figure 3.** Potential energy curves for the  $X^1\Sigma^+$  state of HF computed using various methods and the cc-pVDZ basis set. The upper panel shows the absolute energy, while the lower panel shows the energy deviation from the FCI. All multireference perturbation theories employed a CASSCF(2,2) reference. The fluorine 1s orbital was excluded from the correlation treatment. DSRG-MRPT2 and DSRG-MRPT2 ( $\lambda_3 = 0$ ) employed a flow parameter of  $s = 0.5E_h^{-2}$ , and the MR-MBPT2 curve is identical to the curve of DSRG-MRPT2 ( $s \rightarrow \infty$ ).

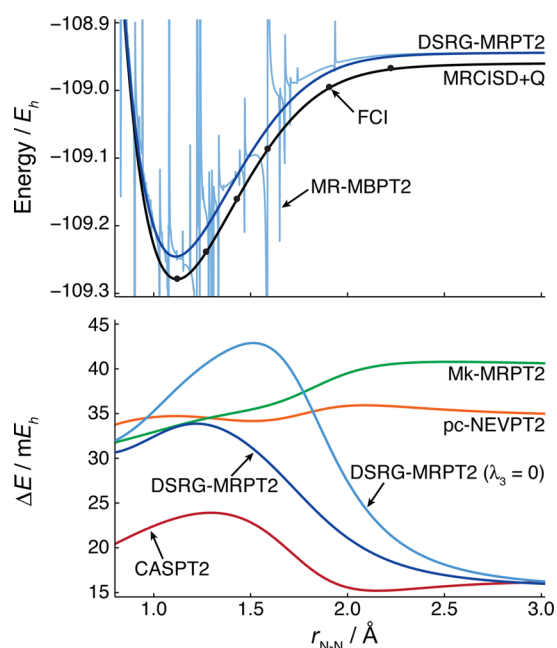


**Figure 4.** Potential energy curves for the  $X^1\Sigma_g^+$  state of  $\text{N}_2$  computed using various methods and the cc-pVDZ basis set. The upper panel shows the absolute potential energy curves, while the lower panel illustrates the energy deviation from the ic-MRCISD+Q. FCI results taken from ref 101 are shown as dots in the top panel. All methods employed a CASSCF(6,6) reference and 1s-like orbitals on nitrogen atoms were excluded from the correlation treatment. DSRG-MRPT2 and DSRG-MRPT2 ( $\lambda_3 = 0$ ) employed a flow parameter of  $s = 0.5E_h^{-2}$ , and the MR-MBPT2 curve is identical to the curve of DSRG-MRPT2 ( $s \rightarrow \infty$ ).



at  $r_{\text{N-N}} = 4.2a_0$ . Potential energy curves for the multireference DSRG-MRPT2 were computed at  $s = 0.5 E_h^{-2}$ , which corresponds to an energy cutoff  $\Lambda = 1.4 E_h$ . We momentarily postpone a more detailed discussion of the choice of  $s$  to section 3.3. However, our choice of the value of  $s$  is consistent with our finding that the optimal range for  $s$  is roughly  $[0.1, 1] E_h^{-2}$ . In addition to the DSRG-MRPT2 energy, we also show the potential curve computed at the MR-MBPT2 level of theory, which is obtained as the  $s \rightarrow \infty$  limit of the DSRG-MRPT2.

For both HF and  $\text{N}_2$ , the DSRG-MRPT2 method yields continuous curves that parallel the benchmark results. On the contrary, it is striking to see that intruders are pervasive in the MR-MBPT2 curves. In the case of HF, intruders significantly shift the energy minimum to longer bond distances. In the case of  $\text{N}_2$ , intruders plague the entire potential energy curve and render it useless. Notice that in the vicinity of the intruders, both the MR-MBPT2 and DSRG-MRPT2 curves were sampled on a very fine grid and that the latter shows no discontinuities. We also note that CASPT2, pc-NEVPT2, and Mk-MRPT2 yield smooth PECs for both the  $X^1\Sigma^+$  state of HF and the  $X^1\Sigma_g^+$  state of  $\text{N}_2$ . It is known in CASPT2 that the choice of zeroth-order Hamiltonian  $[\hat{H}^{(0)}]$  affects the presence of the intruder state.<sup>20</sup> For example, when  $\hat{H}^{(0)}$  is a one-particle Hamiltonian, CASPT2 computations of excited states are prone to the intruder-state problem.<sup>40</sup> Mk-MRPT2 is guaranteed to be free from intruders only for the ground electronic states.<sup>94</sup> In NEVPT2<sup>17,20</sup> the absence of intruders is generally guaranteed by the use of the Dyall Hamiltonian,<sup>103</sup> which contains the active components of the two-body interaction.

The DSRG-MRPT2 is compared to other multireference perturbation theories in the lower panel of Figures 3 and 4, where we plot the energy error ( $\Delta E$ ) computed with respect to the benchmark curves. The DSRG-MRPT2 error remains fairly constant, and the resulting nonparallelism errors (NPEs) are 4.5 and 18.1  $\text{mE}_h$  for HF and  $\text{N}_2$ , respectively. The same figures for pc-NEVPT2 (6.7 and 2.2  $\text{mE}_h$ ), Mk-MRPT2 (4.1 and 9.0  $\text{mE}_h$ ), and CASPT2 (0.2 and 8.7  $\text{mE}_h$ ) show that these methods tend to be more accurate than the DSRG-MRPT2, especially in the case of  $\text{N}_2$ . We also notice that neglecting the three-body cumulant in the DSRG-MRPT2 ( $\lambda_3 = 0$ ), produces potential energy curves of HF and  $\text{N}_2$  with larger absolute errors, especially at intermediate bond lengths. At large bond distances  $\lambda_3$  appears to play a minor role. This is in agreement with prior observations that the odd-rank density cumulants for  $\text{N}_2$  vanish in the limit of infinite bond distance.<sup>104</sup> The NPE for the DSRG-MRPT2 ( $\lambda_3 = 0$ ) method also increases, and it is about twice as large as that of DSRG-MRPT2: 7.7 and 27.1  $\text{mE}_h$  for HF and  $\text{N}_2$ , respectively.

Table 2 reports the spectroscopic constants of HF and  $\text{N}_2$  for different methods obtained by a polynomial fitting of single-point calculations. As in the case of the potential energy curves, our DSRG-MRPT2 theory yields results comparable to those obtained from other second-order perturbation theories. For example, the harmonic frequencies of HF and  $\text{N}_2$  predicted by DSRG-MRPT2 ( $s = 0.5$ ) only differ from the benchmark values by 10.3 and  $-1.3 \text{ cm}^{-1}$ , respectively. Spectroscopic constants are relatively insensitive to the choice of  $s$ : computations that use  $s = 0.5 E_h^{-2}$  and yield results that are in good agreement with the ones obtained using  $s = 0.1$  and  $1.0 E_h^{-2}$ . For  $\text{N}_2$  we notice that the magnitude of the deviation of  $r_e$  and  $\omega_e$  for different values of  $s$  is similar to the one observed in the uncorrected CASPT2 method with a level shift.<sup>40</sup>

**Table 2. Spectroscopic Constants for the  $X^1\Sigma^+$  State of HF and the  $X^1\Sigma_g^+$  State of  $\text{N}_2$  Computed Using Various Methods and the cc-pVDZ Basis Set<sup>a</sup>**

method	$r_e$	$\omega_e$	$\omega_e x_e$
HF			
CASSCF(2,2)	0.0008	−81.3	10.2
CASPT2	0.0000	0.7	−0.1
pc-NEVPT2	0.0035	−15.1	−8.2
Mk-MRPT2	0.0041	−39.5	−6.1
DSRG-MRPT2 (0.1)	−0.0004	24.2	−2.4
DSRG-MRPT2 (0.5)	−0.0026	10.3	1.4
DSRG-MRPT2 (1.0)	−0.0065	15.0	6.4
DSRG-MRPT2 (0.1, $\lambda_3=0$ )	−0.0010	40.3	−3.3
DSRG-MRPT2 (0.5, $\lambda_3=0$ )	−0.0036	38.5	−2.0
DSRG-MRPT2 (1.0, $\lambda_3=0$ )	−0.0075	41.6	1.5
ic-MRCISD+Q	0.0000	−0.8	−0.1
FCI	0.9203	4143.2	92.9
$\text{N}_2$			
CASSCF(6,6)	−0.0060	43.9	−0.3
CASPT2	−0.0012	4.4	0.3
pc-NEVPT2	0.0000	−4.1	0.6
Mk-MRPT2	−0.0012	8.9	0.1
DSRG-MRPT2 (0.1)	−0.0032	23.9	−0.0
DSRG-MRPT2 (0.5)	−0.0013	−1.3	0.7
DSRG-MRPT2 (1.0)	−0.0021	10.0	1.2
DSRG-MRPT2 (0.1, $\lambda_3=0$ )	−0.0046	38.7	−0.1
DSRG-MRPT2 (0.5, $\lambda_3=0$ )	−0.0040	30.5	0.2
DSRG-MRPT2 (1.0, $\lambda_3=0$ )	−0.0045	44.0	0.7
ic-MRCISD+Q	1.1204	2321.4	14.9

<sup>a</sup>Equilibrium distances ( $r_e$ , Å), the harmonic frequencies ( $\omega_e$ ,  $\text{cm}^{-1}$ ), and anharmonicity constants ( $\omega_e x_e$ ,  $\text{cm}^{-1}$ ) are given as deviations from reference values reported at the bottom of each section. The 1s-like molecular orbitals of fluorine and nitrogen were excluded from the correlation treatment. The value of the flow parameter  $s$  used in the DSRG-MRPT2 computations is indicated in parentheses.

Results obtained neglecting the contributions of the three-body cumulants are also reported in Table 2. This approximation slightly deteriorates the quality of the properties, but the largest deviations in bond length and the vibrational frequency are smaller than 0.002 Å and  $20 \text{ cm}^{-1}$ , respectively. This observation suggests that neglecting the three-body cumulant might be a viable approximation that would be especially convenient when treating very large active spaces. However, additional benchmark results are necessary to assess the consequences that neglecting  $\lambda_3$  has on the quality of the DSRG-MRPT2 results.

**3.2. Singlet–Triplet Splittings of  $p$ -Benzynes.** As an example application of the DSRG-MRPT2 to medium-size molecules, we considered the singlet–triplet splitting ( $\Delta E_{\text{ST}}$ ) of  $p$ -benzyne, which has been studied extensively both experimentally<sup>105</sup> and theoretically.<sup>43,47,48,106–111</sup> The simplest active space for such a diradical system is the two-electron in two-orbital complete active space CAS(2,2) that involves only the  $\sigma$  and  $\sigma^*$  orbitals. However, we also report results obtained with an active space that includes the six  $\pi$  orbitals [CAS(8,8)]. To examine the robustness of the current perturbation theory, we employed three values of the flow parameter (0.1, 0.5,  $1.0 E_h^{-2}$ ) and compared the results of DSRG-MRPT2 with other MRPT methods including CASPT2, pc-NEVPT2, and Mk-MRPT2. The singlet and triplet geometries were taken from ref 47 and are shown in Figure 5. These structures were optimized at the



Mk-MRCCSD/cc-pVTZ level of theory using CASSCF(2,2) and ROHF references for the singlet and triplet states, respectively. All computations utilized the cc-pVTZ basis set,<sup>96</sup> and the six 1s-like molecular orbitals on carbon atoms were excluded from the correlation treatment. The computed singlet–triplet splittings include a zero-point vibrational energy (ZPVE) correction (+0.3 kcal mol<sup>−1</sup>) taken from ref 47.

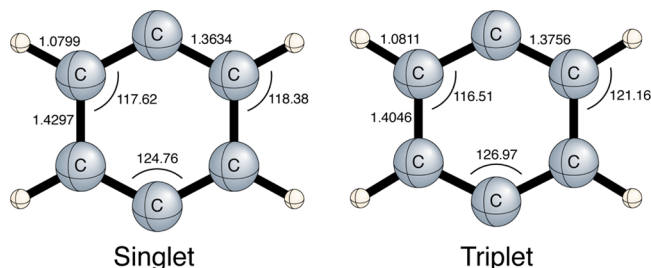


**Figure 5.** Equilibrium structures of *p*-benzyne optimized at the Mk-MRCCSD/cc-pVTZ level of theory in ref 47. Bond lengths are in angstroms, and bond angles are in degrees. The 1s-like molecular orbitals on carbon atoms were kept frozen.

**Table 3. Adiabatic Singlet–Triplet Splittings ( $\Delta E_{\text{ST}}$ , kcal mol<sup>−1</sup>) of *p*-Benzyne Computed Using Various Methods and the cc-pVTZ Basis Set<sup>a</sup>**

method	$\Delta E_{\text{ST}}$
CAS(2,2)	
CASSCF	0.32
CASPT2	4.49
pc-NEVPT2	3.66
Mk-MRPT2	2.44
Mk-MRPT2 (relaxed)	4.91
DSRG-MRPT2 (0.1)	1.25
DSRG-MRPT2 (0.5)	2.62
DSRG-MRPT2 (1.0)	2.96
DSRG-MRPT2 (0.5, $\lambda_3=0$ )	2.10
Mk-MRCCSD <sup>b</sup>	5.20
Mk-MRCCSD(T) <sup>b</sup>	4.45
ic-MRCCSD(T) <sup>c</sup>	5.18
CAS(8,8)	
CASSCF	2.38
CASPT2	5.72
pc-NEVPT2	4.78
DSRG-MRPT2 (0.1)	3.15
DSRG-MRPT2 (0.5)	4.23
DSRG-MRPT2 (1.0)	4.36
DSRG-MRPT2 (0.5, $\lambda_3=0$ )	3.33
expt <sup>d</sup>	3.8 ± 0.4

<sup>a</sup>ZPVE corrections (+0.30 cm<sup>−1</sup>) are included from ref 47. All results used the geometries are taken from ref 47 and are also reported in Figure 5. The value of the flow parameter  $s$  used in the DSRG-MRPT2 computations is indicated in parentheses. <sup>b</sup>From ref 47. <sup>c</sup>From ref 48. <sup>d</sup>From ref 105.

The results of our computations are reported in Table 3. For the small active space, both CASPT2 and pc-NEVPT2 show satisfactory agreement with the photoelectron spectroscopy experiment, while the DSRG-MRPT2 ( $s = 0.5$ ) and Mk-MRPT2 underestimate  $\Delta E_{\text{ST}}$  by more than 1.0 kcal mol<sup>−1</sup>. In the case of Mk-MRPT2, relaxing the reference brings  $\Delta E_{\text{ST}}$  closer to values computed with nonperturbative methods such

as Mk-MRCCSD and ic-MRCCSD(T). The large relaxation effects observed for Mk-MRPT2 suggest that DSRG-MRPT2 might also benefit from the relaxation of the reference. However, as discussed earlier, this introduces some new aspects in the formulation of the theory. The singlet–triplet splitting computed with the DSRG-MRPT2 shows little variation when  $s$  goes from 0.5 to 1.0  $E_h^{-2}$  (2.62 and 2.96 kcal mol<sup>−1</sup>, respectively); however, the value obtained when  $s = 0.1 E_h^{-2}$  is smaller (1.25 kcal mol<sup>−1</sup>). This is likely to be a consequence of the fact that the DSRG transformation computed with  $s = 0.1$  neglects important contributions from low-lying excited configurations that fall under the energy cutoff  $\Lambda = 3.2 E_h$ .

All  $\Delta E_{\text{ST}}$  values increase for the corresponding MRPT methods when employing the larger active space. The DSRG-MRPT2 ( $s = 0.5$ ) method based on a CASSCF(8,8) reference predicts  $\Delta E_{\text{ST}} = 4.23$  kcal mol<sup>−1</sup>, which is in excellent agreement with the  $3.8 \pm 0.4$  kcal mol<sup>−1</sup> experimental estimate. Other MRPT methods yield results that are more in line with the state-of-the-art multireference coupled cluster results. Recent work has shown that the selection of the active space plays a less important role in nonperturbative theories. For example,  $\Delta E_{\text{ST}}$  of *p*-benzyne predicted by the ic-MRCCSD(T) theory with the cc-pVDZ basis set only differs by less than 0.2 kcal mol<sup>−1</sup> between CAS(2,2) and CAS(8,8).<sup>48</sup>

**3.3. Intruder Avoidance and Sensitivity of the Flow Parameter.** In this section, we will discuss how the choice of the flow parameter  $s$  affects the accuracy of the DSRG-MRPT2 energy. Figure 6 shows contour plots of  $\Delta E(r, s)$ , the energy differences between DSRG-MRPT2 and the benchmark methods as a function of the bond distance ( $r$ ) and the flow parameter ( $s$ ). The white region corresponds to  $\Delta E(r, s) = 0$ , while the areas in red and blue show regions where  $\Delta E(r, s)$  is positive and negative, respectively. The magnitude of this energy deviation is proportional to the saturation of the color.

As illustrated in Figure 6, when  $s$  is increased from 0 to about 0.1  $E_h^{-2}$ , the DSRG-MRPT2 gradually includes dynamical correlation effects and the error decreases. For  $s > 10 E_h^{-2}$ , we notice a significant increase in the error and the appearance of valleys and hills. In the limit  $s \rightarrow \infty$ , we observe intruder states appear as an energy denominator becomes singular. An inspection of the contour plots in Figure 6 reveals that when  $s$  is in the range [0.1, 1.0]  $E_h^{-2}$ , the DSRG-MRPT2 shows the smallest absolute error and provides potential energy curves with consistent deviations from the benchmark results.

We conclude this section with a more general discussion of the dependence of the DSRG results with respect to the flow parameter. It is important to point out that, above all, the DSRG is a technique to separate dynamical and static correlation effects. The former are included in the scalar energy  $[E(s)]$ , while the latter are retained in the many-body components of  $\bar{H}(s)$ . Since the DSRG transformation is unitary, when the *exact*  $\bar{H}(s)$  is diagonalized, its eigenvalues will show no dependence on the flow parameter. This discussion leads us to two observations. First, one way to reduce the dependence of the DSRG energy on the value of  $s$  is to retain certain components of  $\bar{H}(s)$  and diagonalize the resulting approximate operator. The partial decoupling achieved by the DSRG transformation implies that as  $s$  grows, the matrix elements between the reference and excited configurations become sparser (for example, see Figure 1). Therefore, the effort required to reintroduce the contributions from near-degenerate configurations that are not included in  $E(s)$  is expected to be

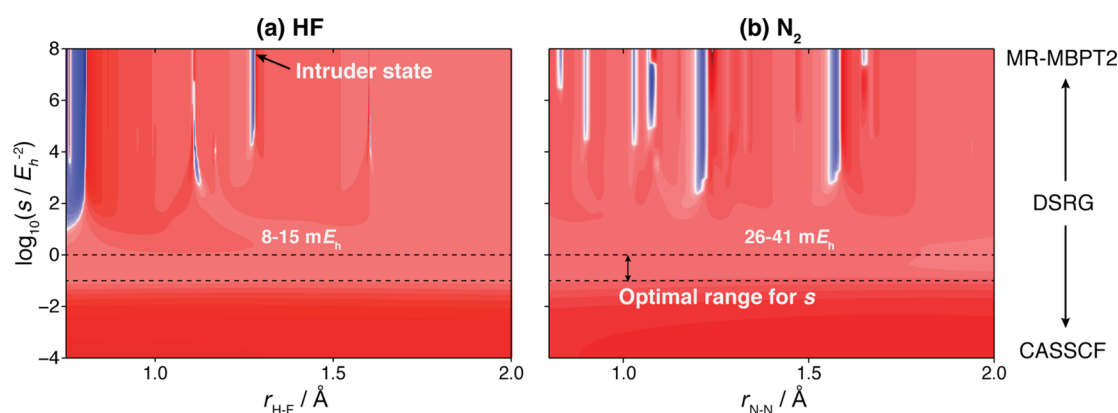


**Figure 6.** Energy error for the DSRG-MRPT2 [ $\Delta E(r,s) = E_{\text{DSRG-MRPT2}}(r,s) - E_{\text{ref}}(r)$ ] for (a) HF against FCI and (b)  $\text{N}_2$  against ic-MRCISD+Q as a function of the bond length ( $r$ ) and flow parameter ( $s$ ). Numerical ranges reported in the plot indicate the lower and upper limits of a contour area. Results were computed using the cc-pVDZ basis set. The CASSCF(2,2) and CASSCF(6,6) references were utilized for HF and  $\text{N}_2$  computations, respectively. The fluorine and nitrogen 1s molecular orbitals were excluded from the correlation treatment.

small. Second, since the perturbative theory derived in this work completely neglects the contributions of  $\bar{H}(s)$ , it provides a way to study the dependence of the DSRG energy on  $s$  in the *worst case scenario*. Our results then provide an upper bound for the dependence of the energy as a function of  $s$ .

#### 4. DISCUSSION AND CONCLUSIONS

This work is a contribution to the development of electron correlation methods based on the renormalization group approach. We have proposed a multireference driven similarity renormalization group (MR-DSRG) theory to account for dynamic electron correlation in near-degenerate electronic states. The multireference DSRG is based on a multi-determinantal reference wave function and uses the generalized operator normal ordering of Mukherjee and Kutzelnigg.<sup>73</sup> The MR-DSRG approach is closely related to internally contracted multireference theories, yet distinct in two crucial aspects. First, the MR-DSRG produces a continuous transformation of the Hamiltonian controlled by a flow parameter ( $s$ ), which can be related to an energy cutoff ( $\Lambda = s^{-1/2}$ ). For finite values of  $s$  the MR-DSRG suppresses those excitations that correspond to a denominator smaller than  $\Lambda$ . This is a common feature of *renormalization group* approaches, and it permits the MR-DSRG to avoid the intruder-state problem. Second, the MR-DSRG is a many-body formalism,<sup>29–31</sup> and as such, it avoids issues connected to linear dependence of the excitation operator found in other internally contracted multireference theories.

As a preliminary study of the MR-DSRG, we derived and implemented a companion second-order perturbation theory (DSRG-MRPT2) based on a CASSCF reference wave function. The DSRG-MRPT2 equations are surprisingly simple. In the semicanonical basis the energy and first-order amplitudes can be obtained via a noniterative procedure, and the DSRG-MRPT2 requires at most the one-particle density matrix to evaluate the amplitudes and the three-particle density cumulant to compute the second-order correlation energy. A formal analysis of the DSRG-MRPT2 equations shows that divergences in the first-order amplitude equations are prevented by a term that regularizes the energy denominators.

A formal argument and a numerical study were used to establish a reliable range of the flow parameter. This is  $s \in [0.1, 1] E_h^{-2}$ , or alternatively when expressed in terms of the energy cutoff,  $\Lambda \in [1, 3] E_h$ . Within this optimal range, the DSRG-MRPT2 gives results that are slightly inferior to those obtained

with other multireference perturbation theories, including CASPT2, pc-NEVPT2, and Mk-MRPT2. For example, the equilibrium distance, the harmonic frequency, and the anharmonicity constant of HF computed at the DSRG-MRPT2 level differ from the FCI figures only by 0.0012 Å, 6.2  $\text{cm}^{-1}$ , and 4.4  $\text{cm}^{-1}$ , respectively. For the adiabatic singlet–triplet splitting ( $\Delta E_{\text{ST}}$ ) of *p*-benzynes, the prediction of DSRG-MRPT2 based on an eight-electron in eight-orbital active space is within 0.5  $\text{kcal mol}^{-1}$  from the experimental value<sup>105</sup> and consistent for values of the flow parameter in the range [0.5, 1.0]  $E_h^{-2}$ . A simplified DSRG-MRPT2 method in which the three-particle cumulant is neglected<sup>30</sup> has also been considered. This approximation reduces the computational complexity of DSRG-MRPT2 [from  $O(N_A^6 N_V)$  to  $O(N_A^4 N_V^2)$ ] without compromising the separability properties of the energy. Our results show that neglecting  $\lambda_3$  increases the nonparallelism error by a factor of 2.

There are several aspects of the DSRG-MRPT2 (and the MR-DSRG) that can be improved and deserve further investigation. Given the fact that the final results are sensitive to the flow parameter used in a calculation, it might be desirable (especially in the case of the DSRG-MRPT2) to seek a procedure that reduces the sensitivity of the final results with respect to  $s$ .<sup>40</sup> We expect the nonperturbative MR-DSRG approach to be less sensitive to intruders. If this is the case, then it will be possible to perform computations with values of  $s$  that are larger than the ones used for the DSRG-MRPT2, and no corrections due to the finite value of  $s$  will be required. Future work will also have to assess if it is possible to formulate improved source operators and, more importantly, find ways to reduce the  $s$ -dependence of the energy by retaining certain components of the DSRG transformed Hamiltonian.

In summary, our analysis of the DSRG-MRPT2 method motivates further developments of the DSRG approach, in particular of the nonperturbative version, which may be a competitor to other internally contracted multireference theories. At the same time this work also suggests several new directions of inquiry. Given the simplicity of the DSRG-MRPT2 equations, this method should easily lend itself to very efficient implementations that take advantage of integral factorization techniques.<sup>112–116</sup> Our results on *p*-benzynes motivate the formulation of the DSRG-MRPT2 with a relaxed reference. It would also be interesting to explore extension of the DSRG-MRPT2 to excited states, in particular to state-

averaged or multistate versions of the theory. These new methods may provide superior results when applied to study potential energy surfaces near conical intersections.

## ■ ASSOCIATED CONTENT

### ● Supporting Information

Text giving a synopsis of the generalized normal ordering and the derivation of the first-order DSRG-MRPT2 amplitudes. This material is available free of charge via the Internet at <http://pubs.acs.org>.

## ■ AUTHOR INFORMATION

### Corresponding Author

\*E-mail: [francesco.evangelista@emory.edu](mailto:francesco.evangelista@emory.edu).

### Funding

This work was supported by start-up funds provided by Emory University. C.L. was supported by National Science Foundation (NSF) Grant CHE-1361178.

### Notes

The authors declare no competing financial interest.

## ■ ACKNOWLEDGMENTS

We thank Dr. David Sherrill, Dr. Justin Turney, and Daniel Smith for the implementation of the CASSCF method in Psi4.

## ■ REFERENCES

- (1) Szalay, P. G.; Müller, T.; Gidofalvi, G.; Lischka, H.; Shepard, R. *Chem. Rev.* **2012**, *112*, 108–181.
- (2) Lyakh, D. I.; Musial, M.; Lotrich, V. F.; Bartlett, R. J. *Chem. Rev.* **2012**, *112*, 182–243.
- (3) Mazziotti, D. A. *Chem. Rev.* **2012**, *112*, 244–262.
- (4) Mok, D. K. W.; Neumann, R.; Handy, N. C. *J. Phys. Chem.* **1996**, *100*, 6225–6230.
- (5) Roos, B. O.; Taylor, P. R.; Siegbahn, P. E. *Chem. Phys.* **1980**, *48*, 157–173.
- (6) White, S. R. *Phys. Rev. Lett.* **1992**, *69*, 2863–2866.
- (7) Chan, G. K.-L.; Head-Gordon, M. *J. Chem. Phys.* **2002**, *116*, 4462–4476.
- (8) Chan, G. K.-L.; Dorando, J.; Ghosh, D.; Hachmann, J.; Neuscamman, E.; Wang, H.; Yanai, T.; An Introduction to the Density Matrix Renormalization Group Ansatz in Quantum Chemistry. In *Frontiers in Quantum Systems in Chemistry and Physics (Progress in Theoretical Chemistry and Physics)*; Wilson, S., Grout, P., Maruani, J., Delgado-Barrio, G., Piecuch, P., Eds.; Springer: Dordrecht, Netherlands, 2008; Vol. 18, pp 49–65.
- (9) Chan, G. K.-L.; Sharma, S. *Annu. Rev. Phys. Chem.* **2011**, *62*, 465–481.
- (10) Casanova, D.; Head-Gordon, M. *Phys. Chem. Chem. Phys.* **2009**, *11*, 9779–9790.
- (11) Zimmerman, P. M.; Bell, F.; Goldey, M.; Bell, A. T.; Head-Gordon, M. *J. Chem. Phys.* **2012**, *137*, 164110.
- (12) Bell, F.; Zimmerman, P. M.; Casanova, D.; Goldey, M.; Head-Gordon, M. *Phys. Chem. Chem. Phys.* **2013**, *15*, 358–366.
- (13) Andersson, K.; Malmqvist, P.-Å.; Roos, B. O.; Sadlej, A. J.; Wolinski, K. *J. Phys. Chem.* **1990**, *94*, 5483–5488.
- (14) Andersson, K.; Malmqvist, P.-Å.; Roos, B. O. *J. Chem. Phys.* **1992**, *96*, 1218–1226.
- (15) Hirao, K. *Chem. Phys. Lett.* **1992**, *190*, 374–380.
- (16) Kozłowski, P. M.; Davidson, E. R. *J. Chem. Phys.* **1994**, *100*, 3672–3682.
- (17) Angeli, C.; Cimiraglia, R.; Evangelista, S.; Leininger, T.; Malrieu, J.-P. *J. Chem. Phys.* **2001**, *114*, 10252–10264.
- (18) Angeli, C.; Cimiraglia, R.; Malrieu, J.-P. *Chem. Phys. Lett.* **2001**, *350*, 297–305.
- (19) Angeli, C.; Cimiraglia, R.; Malrieu, J.-P. *J. Chem. Phys.* **2002**, *117*, 9138–9153.
- (20) Angeli, C.; Pastore, M.; Cimiraglia, R. *Theor. Chem. Acc.* **2007**, *117*, 743–754.
- (21) Chaudhuri, R. K.; Freed, K. F.; Hose, G.; Piecuch, P.; Kowalski, K.; Wloch, M.; Chattopadhyay, S.; Mukherjee, D.; Rolik, Z.; Szabados, Á.; Tóth, G.; Surján, P. R. *J. Chem. Phys.* **2005**, *122*, 134105.
- (22) Knowles, P. J.; Werner, H.-J. *Chem. Phys. Lett.* **1988**, *145*, 514–522.
- (23) Werner, H.-J.; Knowles, P. J. *J. Chem. Phys.* **1988**, *89*, 5803–5814.
- (24) Jezioriski, B.; Monkhorst, H. J. *Phys. Rev. A* **1981**, *24*, 1668–1681.
- (25) Mahapatra, U. S.; Datta, B.; Mukherjee, D. *Mol. Phys.* **1998**, *94*, 157–171.
- (26) Mahapatra, U. S.; Datta, B.; Mukherjee, D. *J. Chem. Phys.* **1999**, *110*, 6171–6188.
- (27) Pittner, J.; Nachtigall, P.; Čársky, P.; Mášik, J.; Hubač, I. *J. Chem. Phys.* **1999**, *110*, 10275–10282.
- (28) Hanrath, M. *J. Chem. Phys.* **2005**, *123*, 084102.
- (29) Kong, L.; Shamasundar, K. R.; Demel, O.; Nooijen, M. *J. Chem. Phys.* **2009**, *130*, 114101.
- (30) Datta, D.; Kong, L.; Nooijen, M. *J. Chem. Phys.* **2011**, *134*, 214116.
- (31) Datta, D.; Nooijen, M. *J. Chem. Phys.* **2012**, *137*, 204107.
- (32) Nooijen, M.; Demel, O.; Datta, D.; Kong, L.; Shamasundar, K. R.; Lotrich, V.; Huntington, L. M.; Neese, F. *J. Chem. Phys.* **2014**, *140*, 081102.
- (33) Yanai, T.; Chan, G. K.-L. *J. Chem. Phys.* **2006**, *124*, 194106.
- (34) Yanai, T.; Chan, G. K.-L. *J. Chem. Phys.* **2007**, *127*, 104107.
- (35) Neuscamman, E.; Yanai, T.; Chan, G. K.-L. *Int. Rev. Phys. Chem.* **2010**, *29*, 231–271.
- (36) Chen, Z.; Hoffmann, M. R. *J. Chem. Phys.* **2012**, *137*, 014108.
- (37) Evangelista, S.; Daudey, J. P.; Malrieu, J.-P. *Phys. Rev. A* **1987**, *35*, 4930–4941.
- (38) Kowalski, K.; Piecuch, P. *Phys. Rev. A* **2000**, *61*, 052506.
- (39) Kowalski, K.; Piecuch, P. *Int. J. Quantum Chem.* **2000**, *80*, 757–781.
- (40) Roos, B. O.; Andersson, K. *Chem. Phys. Lett.* **1995**, *245*, 215–223.
- (41) Witek, H. A.; Choe, Y.-K.; Finley, J. P.; Hirao, K. *J. Comput. Chem.* **2002**, *23*, 957–965.
- (42) Mahapatra, U. S.; Datta, B.; Bandyopadhyay, B.; Mukherjee, D. *Adv. Quantum Chem.* **1998**, *30*, 163–193.
- (43) Evangelista, F. A.; Allen, W. D.; Schaefer, H. F. *J. Chem. Phys.* **2007**, *127*, 024102.
- (44) Banerjee, A.; Simons, J. *Int. J. Quantum Chem.* **1981**, *19*, 207–216.
- (45) Evangelista, F. A.; Gauss, J. *J. Chem. Phys.* **2011**, *134*, 114102.
- (46) Hanauer, M.; Köhn, A. *J. Chem. Phys.* **2011**, *134*, 204111.
- (47) Evangelista, F. A.; Hanauer, M.; Köhn, A.; Gauss, J. *J. Chem. Phys.* **2012**, *136*, 204108.
- (48) Hanauer, M.; Köhn, A. *J. Chem. Phys.* **2012**, *136*, 204107.
- (49) Köhn, A.; Hanauer, M.; Mück, L. A.; Jagau, T.-C.; Gauss, J. *WIREs: Comput. Mol. Sci.* **2013**, *3*, 176–197.
- (50) Lindgren, I. *Int. J. Quantum Chem.* **1978**, *14*, 33–58.
- (51) Nooijen, M.; Bartlett, R. J. *J. Chem. Phys.* **1996**, *104*, 2652–2668.
- (52) Hachmann, J.; Dorando, J. J.; Avilés, M.; Chan, G. K.-L. *J. Chem. Phys.* **2007**, *127*, No. 134309.
- (53) Mizukami, W.; Kurashige, Y.; Yanai, T. *J. Chem. Theory Comput.* **2013**, *9*, 401–407.
- (54) Kurashige, Y.; Chan, G. K.-L.; Yanai, T. *Nat. Chem.* **2013**, *5*, 660–666.
- (55) Evangelista, F. A. *J. Chem. Phys.* **2014**, *141*, 054109.
- (56) Glazek, S. D.; Wilson, K. G. *Phys. Rev. D* **1993**, *48*, 5863–5872.
- (57) Glazek, S. D.; Wilson, K. G. *Phys. Rev. D* **1994**, *49*, 4214–4218.
- (58) Wegner, F. *Ann. Phys. (Leipzig)* **1994**, *3*, 77–91.
- (59) Wegner, F. Flow Equations for Hamiltonians. In *Advances in Solid State Physics*; Kramer, B., Ed.; Springer: Berlin, Heidelberg, 2000; Vol. 40, pp 133–142.
- (60) White, S. R. *J. Chem. Phys.* **2002**, *117*, 7472–7482.



- (61) Kehrein, S. *The Flow Equation Approach to Many-Particle Systems*; Springer: Berlin, Heidelberg, 2006.
- (62) Roth, R.; Reinhardt, S.; Hergert, H. *Phys. Rev. C* **2008**, *77*, 064003.
- (63) Hergert, H.; Bogner, S. K.; Binder, S.; Calci, A.; Langhammer, J.; Roth, R.; Schwenk, A. *Phys. Rev. C* **2013**, *87*, 034307.
- (64) Furnstahl, R. J.; Hebeler, K. *Rep. Prog. Phys.* **2013**, *76*, 126301.
- (65) Hergert, H.; Binder, S.; Calci, A.; Langhammer, J.; Roth, R. *Phys. Rev. Lett.* **2013**, *110*, 242501.
- (66) Purvis, G. D.; Bartlett, R. J. *J. Chem. Phys.* **1982**, *76*, 1910–1918.
- (67) Crawford, T. D.; Schaefer, H. F. *Rev. Comput. Chem.* **2000**, *14*, 33–136.
- (68) Bartlett, R. J.; Musial, M. *Rev. Mod. Phys.* **2007**, *79*, 291–352.
- (69) Raghavachari, K.; Trucks, G. W.; Pople, J. A.; Head-Gordon, M. *Chem. Phys. Lett.* **1989**, *157*, 479–483.
- (70) Bartlett, R. J.; Watts, J.; Kucharski, S.; Noga, J. *Chem. Phys. Lett.* **1990**, *165*, 513–522.
- (71) Deegan, M. J.; Knowles, P. J. *Chem. Phys. Lett.* **1994**, *227*, 321–326.
- (72) Stanton, J. F. *Chem. Phys. Lett.* **1997**, *281*, 130–134.
- (73) Kutzelnigg, W.; Mukherjee, D. *J. Chem. Phys.* **1997**, *107*, 432–449.
- (74) Kutzelnigg, W.; Mukherjee, D. *J. Chem. Phys.* **1999**, *110*, 2800–2809.
- (75) Mazziotti, D. A. *Phys. Rev. Lett.* **2006**, *97*, 143002.
- (76) Mazziotti, D. A. *Phys. Rev. A* **2007**, *75*, 022505.
- (77) Jeffcoat, D. B.; DePrince, A. E. *J. Chem. Phys.* **2014**, *141*, 214104.
- (78) Mukherjee, D. *Chem. Phys. Lett.* **1997**, *274*, 561–566.
- (79) Sinha, D.; Maitra, R.; Mukherjee, D. *Comput. Theor. Chem.* **2013**, *1003*, 62–70.
- (80) Kutzelnigg, W. *Int. J. Quantum Chem.* **2009**, *109*, 3858–3884.
- (81) Kutzelnigg, W. Unconventional Aspects in Coupled-Cluster Theory. In *Recent Progress in Coupled Cluster Methods (Challenges and Advances in Computational Chemistry and Physics)*; Čársky, P., Paldus, J., Pittner, J., Eds.; Vol. 11 Springer: Dordrecht, Netherlands, 2010; pp 299–356.
- (82) Shamasundar, K. R. *J. Chem. Phys.* **2009**, *131*, 174109.
- (83) Kong, L.; Nooijen, M.; Mukherjee, D. *J. Chem. Phys.* **2010**, *132*, 234107.
- (84) Evangelista, F. A.; Gauss, J. *Chem. Phys.* **2012**, *401*, 27–35.
- (85) Handy, N. C.; Pople, J. A.; Head-Gordon, M.; Raghavachari, K.; Trucks, G. W. *Chem. Phys. Lett.* **1989**, *164*, 185–192.
- (86) Lauderdale, W. J.; Stanton, J. F.; Gauss, J.; Watts, J. D.; Bartlett, R. J. *Chem. Phys. Lett.* **1991**, *187*, 21–28.
- (87) Brandow, B. *Rev. Mod. Phys.* **1967**, *39*, 771–828.
- (88) Amos, R. D.; Andrews, J. S.; Handy, N. C.; Knowles, P. J. *Chem. Phys. Lett.* **1991**, *185*, 256–264.
- (89) Taube, A. G.; Bartlett, R. J. *J. Chem. Phys.* **2009**, *130*, 144112.
- (90) Ohnishi, Y.-y.; Ishimura, K.; Ten-no, S. *J. Chem. Theory Comput.* **2014**, *10*, 4857–4861.
- (91) Hanrath, M. *Chem. Phys.* **2009**, *356*, 31–38.
- (92) Hanauer, M.; Köhn, A. *J. Chem. Phys.* **2012**, *137*, 131103.
- (93) Celani, P.; Werner, H.-J. *J. Chem. Phys.* **2000**, *112*, 5546–5557.
- (94) Evangelista, F. A.; Simmonett, A. C.; Schaefer, H. F.; Mukherjee, D.; Allen, W. D. *Phys. Chem. Chem. Phys.* **2009**, *11*, 4728–4741.
- (95) Langhoff, S. R.; Davidson, E. R. *Int. J. Quantum Chem.* **1974**, *8*, 61–72.
- (96) Dunning, T. H. *J. Chem. Phys.* **1989**, *90*, 1007–1023.
- (97) Turney, J. M.; Simmonett, A. C.; Parrish, R. M.; Hohenstein, E. G.; Evangelista, F. A.; Fermann, J. T.; Mintz, B. J.; Burns, L. A.; Wilke, J. J.; Abrams, M. L.; Russ, N. J.; Leininger, M. L.; Janssen, C. L.; Seidl, E. T.; Allen, W. D.; Schaefer, H. F.; King, R. A.; Valeev, E. F.; Sherrill, C. D.; Crawford, T. D. *WIREs: Comput. Mol. Sci.* **2012**, *2*, 556–565.
- (98) Werner, H.-J.; Knowles, P. J. *J. Chem. Phys.* **1985**, *82*, 5053–5063.
- (99) Knowles, P. J.; Werner, H.-J. *Chem. Phys. Lett.* **1985**, *115*, 259–267.
- (100) Werner, H.-J.; Knowles, P. J.; Knizia, G.; Manby, F. R.; Schütz, M.; Celani, P.; Korona, T.; Lindh, R.; Mitrushenkov, A.; Rauhut, G.; Shamasundar, K. R.; Adler, T. B.; Amos, R. D.; Bernhardsson, A.; Berning, A.; Cooper, D. L.; Deegan, M. J. O.; Dobbyn, A. J.; Eckert, F.; Goll, E.; Hampel, C.; Hesselmann, A.; Hetzer, G.; Hrenar, T.; Jansen, G.; Köppl, C.; Liu, Y.; Lloyd, A. W.; Mata, R. A.; May, A. J.; McNicholas, S. J.; Meyer, W.; Mura, M. E.; Nicklass, A.; O'Neill, D. P.; Palmieri, P.; Pflüger, K.; Pitzer, R.; Reiher, M.; Shiozaki, T.; Stoll, H.; Stone, A. J.; Tarroni, R.; Thorsteinsson, T.; Wang, M.; Wolf, A. *MOLPRO*, version 2010.1, a package of *ab initio* programs; see <http://www.molpro.net>. 2010.
- (101) Chan, G. K.-L.; Kállay, M.; Gauss, J. *J. Chem. Phys.* **2004**, *121*, 6110–6116.
- (102) Bauschlicher, C. W.; Taylor, P. R. *Theor. Chim. Acta* **1987**, *71*, 263–276.
- (103) Dyall, K. G. *J. Chem. Phys.* **1995**, *102*, 4909–4918.
- (104) Hanauer, M.; Köhn, A. *Chem. Phys.* **2012**, *401*, 50–61.
- (105) Wenthold, P. G.; Squires, R. R.; Lineberger, W. C. *J. Am. Chem. Soc.* **1998**, *120*, 5279–5290.
- (106) Li, X.; Paldus, J. *J. Chem. Phys.* **2008**, *129*, 174101.
- (107) Cramer, C. J.; Nash, J. J.; Squires, R. R. *Chem. Phys. Lett.* **1997**, *277*, 311–320.
- (108) Lindh, R.; Bernhardsson, A.; Schütz, M. *J. Phys. Chem. A* **1999**, *103*, 9913–9920.
- (109) Slipchenko, L. V.; Krylov, A. I. *J. Chem. Phys.* **2002**, *117*, 4694–4708.
- (110) Li, H.; Yu, S.-Y.; Huang, M.-B.; Wang, Z.-X. *Chem. Phys. Lett.* **2007**, *450*, 12–18.
- (111) Wang, E. B.; Parish, C. A.; Lischka, H. *J. Chem. Phys.* **2008**, *129*, 044306.
- (112) Weigend, F.; Kattannek, M.; Ahlrichs, R. *J. Chem. Phys.* **2009**, *130*, 164106.
- (113) Aquilante, F.; Malmqvist, P.-Å.; Pedersen, T. B.; Ghosh, A.; Roos, B. O. *J. Chem. Theory Comput.* **2008**, *4*, 694–702.
- (114) DePrince, A. E.; Sherrill, C. D. *J. Chem. Theory Comput.* **2013**, *9*, 2687–2696.
- (115) Epifanovsky, E.; Zuev, D.; Feng, X.; Khistyayev, K.; Shao, Y.; Krylov, A. I. *J. Chem. Phys.* **2013**, *139*, 134105.
- (116) Györfy, W.; Shiozaki, T.; Knizia, G.; Werner, H.-J. *J. Chem. Phys.* **2013**, *138*, 104104.